Synthesis and Initial in Vitro Evaluations of Novel Antioxidant Aroylhydrazone Iron Chelators with Increased Stability against Plasma Hydrolysis

ARTICLE *in* CHEMICAL RESEARCH IN TOXICOLOGY · MARCH 2011

Impact Factor: 3.53 · DOI: 10.1021/tx100359t · Source: PubMed

9 AUTHORS, INCLUDING:

Katerina Hrusková
Charles University in Prague
3 PUBLICATIONS **31** CITATIONS
SEE PROFILE

Pavlina Haskova
Charles University in Prague
26 PUBLICATIONS **298** CITATIONS
SEE PROFILE

Anna Jirkovska
Charles University in Prague
18 PUBLICATIONS **229** CITATIONS
SEE PROFILE

Katerina Vávrová
Charles University in Prague
73 PUBLICATIONS **896** CITATIONS
SEE PROFILE

Chemical Research in Toxicology

ARTICLE

pubs.acs.org/crt

Synthesis and Initial *in Vitro* Evaluations of Novel Antioxidant Aroylhydrazone Iron Chelators with Increased Stability against Plasma Hydrolysis

Katerina Hruskova, Petra Kovarikova, Petra Bendova, Pavlina Haskova, Eliska Mackova, Jan Stariat, Anna Vavrova, Katerina Vavrova,* and Tomas Simunek*

Faculty of Pharmacy in Hradec Kralove, Charles University in Prague, Czech Republic

ABSTRACT: Oxidative stress is known to contribute to a number of cardiovascular pathologies. Free intracellular iron ions participate in the Fenton reaction and therefore substantially contribute to the formation of highly toxic hydroxyl radicals and cellular injury. Earlier work on the intracellular iron chelator salicylaldehyde isonicotinoyl hydrazone (SIH) has demonstrated its considerable promise as an agent to protect the heart against oxidative injury both *in vitro* and *in vivo*. However, the major limitation of SIH is represented by its labile hydrazone bond that makes it prone to plasma hydrolysis. Hence, in order to improve the hydrazone bond stability, nine compounds were prepared by a substitution of salicylaldehyde by the respective methyl- and ethylketone with various electron donors or acceptors in the phenyl ring. All the synthesized aroylhydrazones displayed significant iron-chelating activities and eight chelators showed significantly higher stability in rabbit plasma than SIH. Furthermore, some of these chelators were observed to possess higher cytoprotective activities against oxidative injury and/or lower toxicity as compared to SIH. The results of the present study therefore indicate the possible applicability of several of these novel agents in the prevention and/or treatment of cardiovascular disorders with a known (or presumed) role of oxidative stress. In particular, the methylketone HAPI and nitro group-containing NHAPI merit further *in vivo* investigations.

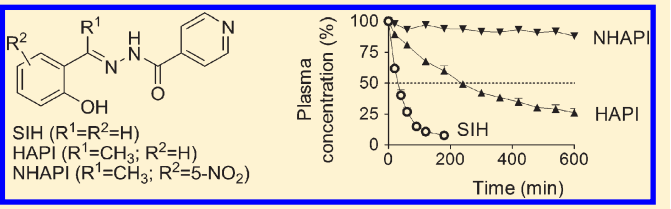

INTRODUCTION

An imbalance in cellular redox state, in which the production of reactive oxygen species (ROS) overwhelms antioxidant capacity, results in the state termed oxidative stress.[1] Recent evidence suggests that oxidative stress is a common denominator in many aspects of cardiovascular pathogenesis. Its important role is now established in ischemia-reperfusion myocardial injury, cardiac arrhythmias, congestive heart failure, myocarditis, anthracycline-induced cardiomyopathy, atherosclerosis, or hypertension.[1−3]

Iron (Fe) is an essential element for all living cells. However, unless appropriately complexed, this transition metal may catalyze the Fenton reaction which results in the formation of extremely reactive and toxic hydroxyl radicals that readily attack various biological molecules. Therefore, organisms are equipped with specific proteins designed for Fe acquisition, transport, and storage, as well as with sophisticated mechanisms that maintain the intracellular labile iron pool (LIP) at an appropriate level. Despite these homeostatic regulations, under certain pathological states, cells face the threat of Fe toxicity. High cellular levels of superoxide and peroxide species, as well as low pH (e.g., during ischemia), are able to release Fe from its storage proteins, increase the redox-active LIP, and thus further promote the production of ROS.[4,5]

Despite the well-known pathophysiological role of ROS, conventional treatment of cardiovascular diseases still lacks the use of antioxidants due to negative study outcomes. Unfortunately, efforts to reduce oxidative stress have focused primarily on the use of ROS scavengers, rather than on actual prevention of ROS production. The latter can be achieved with Fe-chelating agents, which have been clinically used for the reduction of excessive body iron accumulation in disorders such as β-thalassemia.[6,7] Here, effective Fe chelation has been particularly beneficial due to the reduction of cardiac mortality caused by excessive myocardial Fe loading and prevention of ROS-mediated myocardial damage.[8] Besides the Fe-overloading conditions, a growing body of evidence suggests that the concept of Fe chelation may also be useful in preventing Fe-mediated aggravation of oxidative stress, which can occur locally even in the presence of normal body Fe stores.[9] Indeed, the clinically approved agent dexrazoxane (ICRF-187) is supposed to reduce the cardiotoxicity of redox-cycling anthracycline anticancer drugs by binding free cellular Fe and preventing site-specific oxidative stress within cardiac tissue.[10]

Salicylaldehyde isonicotinoyl hydrazone (SIH) is a tridental chelator selectively forming 2:1 complexes with Fe^{3+}. Because of its low molecular weight and optimal lipophilicity, SIH can be administered orally. It readily enters the cells, firmly chelates the intracellular LIP, and is therefore able to very efficiently block the Fe-dependent production of hydroxyl radicals. SIH has been previously shown as very effective in the protection of guinea pig or rat isolated cardiomyocytes and H9c2 cells as well as other cell types against the H_2O_2-induced cell injury, apparently due to the

Received: October 21, 2010
Published: January 07, 2011

preservation of mitochondrial function and/or lysosomal integrity.[11−14] SIH also efficiently protected H9c2 cells against oxidative injury induced by *tert*-butyl hydroperoxide.[15] In the latter study, SIH showed the best ratio of cytoprotective efficiency and own inherent toxicity of seven Fe chelating agents from several distinct chemical families including three clinically used drugs: the bacterial siderophore desferrioxamine (DFO), hydroxypyridinone deferiprone (L1, CP20) and triazole deferasirox (ICL670A).[15] In addition, SIH has also been shown to efficiently protect against the cardiotoxicity of anthracycline daunorubicin, both *in vitro* using isolated neonatal rat cardiomyocytes[16] and *in vivo* using the chronic rabbit model of anthracycline-induced heart failure.[17] A recent study demonstrated marked protective efficiency of SIH against cellular injury by gamma irradiation.[18] Low *in vivo* toxicity and good tolerability of SIH has been demonstrated following its 10-week repeated administration to rabbits.[19] Furthermore, aroylhydrazone pro-chelators have been recently developed in which the Fe-binding groups are chemically masked, and the active chelator SIH is generated only at sites of ROS production.[20−22]

Despite these promising pharmacodynamic findings, a pilot pharmacokinetic study of SIH has revealed the relatively short biological half-life of this drug candidate following its single intravenous administration to rabbits,[23] apparently due to its labile hydrazone bond which makes the molecule prone to hydrolysis.[23−25] Other studies showed that this feature is not specific for SIH; it is rather a class effect of all aroylhydrazones formed by the coupling of isoniazide with aromatic aldehydes.[26,27] Such rapid plasma clearance results in a need for large bolus doses with transient very high peak plasma concentrations, which may have been responsible for the reduction of cardioprotective effectiveness of SIH upon dose escalation.[28] Hence, although SIH has been shown to be effective and safe, the pharmacokinetic weakness may represent a serious obstacle for its further development and potential use in clinical practice. Therefore, the improvement of the plasma stability of SIH through modification of its chemical structure may strengthen the therapeutic potential of this class of compounds.

Our ultimate goal is to find an effective chelator with low toxicity and improved hydrolytic stability compared to those of SIH. The aim of this first initial study was to synthesize and screen a series of SIH-derived aroylhydrazones in order to identify the variables that determine their hydrolytic stability. At the same time, we aimed at studying the Fe-chelating properties of the evaluated agents in solution and access to LIP in the cardiac-derived cell line H9c2, and *in vitro* assessments of cellular protective actions of the chelators against model oxidative injury as well as determinations of the individual toxicities of these substances.

EXPERIMENTAL PROCEDURES

Syntheses of Chelators. All chemicals were purchased from Sigma-Aldrich (Schnelldorf, Germany). Thin layer chromatography was performed on TLC sheets (silica gel 60 F_{254}) from Merck (Darmstadt, Germany). Microwave reactions were conducted in a Milestone Micro-SYNTH Ethos 1600 URM apparatus. Melting points were measured on a Kofler apparatus and are uncorrected. All products were characterized by IR (Nicolet Impact 400 spectrophotometer) and NMR (Varian Mercury-Vx BB 300 instrument, ^{1}H at 300 MHz and ^{13}C at 75 MHz) spectra. The reference chelator SIH was synthesized as described previously.[29]

(*E*)-*N*′-[1-(2-Hydroxyphenyl)ethyliden]isonicotinoylhydrazide (HAPI). Isoniazid (0.54 g, 3.9 mmol), 2-hydroxyacetophenone (0.53 g, 3.9 mmol), and acetic acid (1 mL, 17.5 mmol) in 48% ethanol (10 mL) were stirred under reflux for 9 h. After cooling the reaction mixture to room temperature (RT), we added H_2O (10 mL), and the mixture was allowed to crystallize at 4 °C. The product was collected by filtration, washed with H_2O, and dried over P_2O_5 under reduced pressure to give 0.77 g (77%) of yellowish crystals, mp 240−242 °C (lit.[30] 235−237 °C). ^{1}H NMR (300 MHz, Me_2SO): δ 13.19 (1H; s; OH); 11.59 (1H; s; NH); 8.79 (2H; d; J = 4.4 Hz; Py); 7.84 (2H; d; J = 5.3 Hz; Py); 7.65 (1H; d; J = 7.6 Hz; Ph); 7.32 (1H; dd; J = 5.9 Hz; J = 7.6 Hz; Ph); 6.92 (1H; d; J = 8.2 Hz; Ph); 6.89 (1H; d; J = 7.8 Hz; Ph); 2.49 (3H; s; CH_3). ^{13}C NMR (75 MHz, Me_2SO): δ 163.2; 159.7; 159.0; 150.4; 140.3; 131.8; 129.0; 122.2; 119.4; 118.8; 117.6; 14.5. IR (KBr): ν_{max} 3436; 3116; 1681; 1642; 1610; 1535; 1495; 1304; 1298 cm^{-1}.

(*E*)-*N*′-[1-(2-Hydroxyphenyl)propyliden]isonicotinoylhydrazide (HPPI). Isoniazid (0.255 g, 1.9 mmol) and 2-hydroxypropiophenone (0.28 g, 1.9 mmol) in 96% ethanol (5 mL) were stirred under reflux in a microwave reactor (400 W) for 30 min. Then, acetic acid (0.25 mL, 4.4 mmol) was added and the reaction continued for a further 30 min. The reaction mixture was allowed to crystallize at 4 °C. The solid was filtered, washed with H_2O, and recrystallized from ethanol to yield 0.24 g (48%) of yellowish crystals, mp 244−246 °C (lit.[31] 248 °C). ^{1}H NMR (300 MHz, Me_2SO): δ 13.28 (1H; s; OH); 11.61 (1H; s; NH); 8.79 (2H; d; J = 5.9 Hz; Py); 7.80 (2H; d; J = 5.5 Hz; Py); 7.64 (1H; d; J = 7.5 Hz; Ph); 7.31 (1H; dd; J = 8.4 Hz; J = 7.2 Hz; Ph); 6.92 (1H; d; J = 8.3 Hz; Ph); 6.89 (1H; d; J = 7.2 Hz; Ph); 3.01 (2H; q; J = 7.6 Hz; CH_2); 1.14 (3H; t; J = 7.6 Hz; CH_3). ^{13}C NMR (75 MHz, Me_2SO): δ 163.6; 162.7; 159.5; 150.3; 140.5; 131.7; 128.6; 122.4; 118.9; 117.9; 117.9; 19.6; 11.6. IR (KBr): ν_{max} 3436; 3139; 1683; 1603; 1528; 1488; 1279 cm^{-1}.

(*E*)-*N*′-[1-(2,4-Dihydroxyphenyl)ethyliden]isonicotinoylhydrazide (2,4DHAPI). Isoniazid (0.51 g, 3.7 mmol), 2,4-dihydroxyacetophenone (0.56 g, 3.7 mmol), and acetic acid (1 mL, 17.5 mmol) in 96% ethanol (10 mL) were stirred under reflux for 9 h. The reaction mixture was cooled to RT, and after addition of H_2O (10 mL), the product was obtained by filtration and washed with H_2O. Recrystallization from ethanol gave 0.35 g (35%) of yellowish crystals, mp 284−286 °C. ^{1}H NMR (300 MHz, Me_2SO): δ 13.38 (2H; s; OH); 11.41 (1H; s; NH); 8.78 (2H; d; J = 5.6 Hz; Py); 7.82 (2H; d; J = 5.8 Hz; Py); 7.46 (1H; s; Ph); 6.40−6.35 (1H; m; Ph); 6.30−6.25 (1H; m; Ph); 2.41 (3H; s; CH_3). ^{13}C NMR (75 MHz, Me_2SO): δ 162.8; 161.1; 160.9; 160.7; 150.4; 140.5; 130.4; 111.6; 107.2; 103.4; 14.4. IR (KBr): ν_{max} 3525; 3087; 1671; 1617; 1507; 1328; 1271 cm^{-1}.

(*E*)-*N*′-[1-(2,6-Dihydroxyphenyl)ethyliden]isonicotinoylhydrazide (2,6DHAPI). Isoniazid (0.28 g, 2 mmol), 2,6-dihydroxyacetophenone (0.255 g, 1.7 mmol), and acetic acid (0.25 mL, 4.4 mmol) in 96% ethanol (5 mL) were stirred under reflux in a microwave reactor (400 W) for 5 h. After cooling the reaction mixture to RT, the resulting product was filtered off, washed with H_2O, and dried over P_2O_5 affording 0.132 g (26%) of yellowish crystals, mp 245−247 °C. ^{1}H NMR (300 MHz, Me_2SO): δ 11.41 (2H; s; OH); 11.06 (1H; s; NH); 8.78 (2H; d; J = 4.3 Hz; Py); 7.83 (2H; d; J = 4.3 Hz; Py); 7.05−7.00 (1H; m; Ph); 6.37 (2H; d; J = 8.1 Hz; Ph); 2.45 (3H; s; CH_3). ^{13}C NMR (75 MHz, Me_2SO): δ 162.9; 161.3; 158.2; 150.4; 140.5; 131.3; 122.1; 110.5; 107.4; 19.4. IR (KBr): ν_{max} 3369; 3173; 1656; 1603; 1529; 1450; 1286 cm^{-1}.

(*E*)-*N*′-[1-(2-Hydroxy-4-methoxyphenyl)ethyliden]isonicotinoylhydrazide (MHAPI). Isoniazid (0.53 g, 3.9 mmol), 2-hydroxy-4-methoxyacetophenone (0.64 g, 3.9 mmol), and acetic acid (0.2 mL, 3.5 mmol) in 96% ethanol (10 mL) were stirred under reflux in a microwave reactor (400 W) for 2 h. The reaction mixture was cooled to 4 °C. The resulting product was filtered, washed with H_2O, and dried over P_2O_5 giving 0.24 g (24%) of yellowish crystals, mp 219−222 °C. ^{1}H NMR (300 MHz, Me_2SO): δ 13.51 (1H; s; OH); 11.47 (1H; s; NH); 8.74 (2H; d; J = 5.9 Hz; Py); 7.83 (2H; d; J = 6.0 Hz; Py); 7.56 (1H; d; J = 8.4 Hz; Ph); 6.50 (2H; d; J = 2.6 Hz; Ph); 6.47 (1H; s; Ph); 3.77 (s; OCH_3); 2.45 (3H; s; CH_3). ^{13}C NMR (75 MHz, Me_2SO): δ 162.9; 162.2; 161.1; 160.1; 150.4; 140.4; 130.2; 122.2; 112.7; 106.1; 101.7; 55.5; 14.4. IR (KBr): ν_{max} 3346; 3150; 1678; 1618; 1511; 1264; 1138 cm^{-1}.

(*E*)-*N*′-[1-(5-Chloro-2-hydroxyphenyl)ethyliden]isonicotinoylhydrazide (CHAPI). Isoniazid (0.24 g, 1.8 mmol) and 5-chloro-2-hydroxyacetophenone (0.29 g, 1.7 mmol) in 96% ethanol (5 mL) were stirred under reflux in a microwave reactor (200 W) for 1 h. Acetic acid (0.25 mL, 4.4 mmol) was added and the reaction continued for a further 1 h. The resulting solid was filtered and washed with H_2O. The filtrate was collected and cooled overnight at 4 °C to obtain another portion of product. The combined solids were recrystallized from ethanol and dried over P_2O_5 affording 0.23 g (46%) of yellowish crystals, mp 236−238 °C (lit. 242 °C[31]). ^{1}H NMR (300 MHz, Me_2SO): δ 13.26 (1H; s; OH); 11.66 (1H; s; NH); 8.79 (2H; d; J = 5.6 Hz; Py); 7.84 (2H; d; J = 6.0 Hz; Py); 7.66 (1H; d; J = 2.6 Hz; Ph); 7.34 (1H; dd; J = 2.6 Hz; Ph); 6.95 (1H; d; J = 8.8 Hz; Ph); 2.49 (3H; s; CH_3). ^{13}C NMR (75 MHz, Me_2SO): δ 163.4; 158.2; 157.6; 150.4; 140.1; 131.3; 128.2; 122.4; 122.3; 120.9; 119.4; 14.6. IR (KBr): ν_{max} 3443; 3177; 1682; 1602; 1527; 1289; 675 cm^{-1}.

(*E*)-*N*′-[1-(2-Hydroxy-5-nitrophenyl)ethyliden]isonicotinoylhydrazide (NHAPI). Isoniazid (0.23 g, 1.7 mmol) and 2-hydroxy-5-nitroacetophenone (0.31 g, 1.7 mmol) in 96% ethanol (5 mL) were stirred at reflux in a microwave reactor (400 W) for 1 h. After the mixture was cooled to 4 °C, the resulting product was obtained by filtration and washed with H_2O. The recrystallization from ethanol gave 0.317 g (63%) of orange crystals, mp 274−276 °C. ^{1}H NMR (300 MHz, Me_2SO): δ 14.39 (1H; s; OH); 11.86 (1H; s; NH); 8.80 (2H; d; J = 5.7 Hz; Py); 8.46 (2H; d; J = 2.8 Hz; Py); 8.21−8.17 (1H; m; Ph); 7.90−7.85 (1H; m; Ph); 7.11 (1H; d; J = 9.1 Hz; Ph); 2.56 (3H; s; CH_3). ^{13}C NMR (75 MHz, Me_2SO): δ 164.6; 163.6; 157.5; 150.4; 139.9; 139.3; 127.0; 125.0; 122.3; 119.5; 118.6; 14.6. IR (KBr): ν_{max} 3458; 3146; 1661; 1614; 1516; 1289 cm^{-1}.

(*E*)-*N*′-[1-(5-Acetyl-2,4-dixydroxyphenyl)ethyliden]isonicotinoylhydrazide (A2,4DHAPI). Isoniazid (0.22 g, 1.6 mmol), 2,4-diacetylresorcinol (0.31 g, 1.6 mmol), and acetic acid (0.5 mL, 8.8 mmol) in 96% ethanol (5 mL) were stirred at reflux in a microwave reactor for 2.5 h. After cooling the reaction mixture to 4 °C, the resulting solid was filtered, washed with H_2O, and recrystallized from ethanol to give 0.437 g (87%) of orange crystals, mp 294−300 °C. ^{1}H NMR (300 MHz, Me_2SO): δ 14.33 (1H; s; OH); 12.61 (1H; s; OH); 11.62 (1H; s; NH); 8.78 (2H; d; J = 4.4 Hz; Py); 8.10 (1H; s; Ph); 7.83 (2H; d; J = 6.0 Hz; Py); 6.36 (1H; s; Ph); 2.64 (3H; s; CH_3); 2.54 (3H; s; CH_3). ^{13}C NMR (75 MHz, Me_2SO): δ 203.0; 166.0; 164.6; 163.2; 159.2; 150.4; 140.1; 133.9; 122.2; 113.5; 112.8; 104.0; 27.2; 14.4. IR (KBr): ν_{max} 3447; 3131; 1682; 1645; 1585; 1263 cm^{-1}.

(*E*)-*N*′-(1-(7-Hydroxy-2-oxo-2*H*-chromen-8-yl)ethylidene)isonicotinohydrazide (AHCI). Isoniazid (0.21 g, 1.5 mmol) and 8-acetyl-7-hydroxycoumarine (0.32 g, 1.6 mmol) in 96% ethanol (5 mL) were stirred at reflux in microwave reactor (400 W) for 20 min. The product was filtered off, washed with H_2O, and dried over P_2O_5 to give 0.303 g (61%) of yellowish crystals, mp 327−330 °C. ^{1}H NMR (300 MHz, Me_2SO): δ 11.90 (1H; s; OH); 11.40 (1H; s; NH); 8.78 (2H; d; J = 5.2 Hz; Py); 7.98 (2H; d; J = 9.5 Hz; Py); 7.83 (1H; d; J = 5.4 Hz; Naph); 7.59 (1H; d; J = 8.6 Hz; Naph); 6.93 (1H; d; J = 8.5 Hz; Naph); 6.25 (1H; d; J = 9.5 Hz; Naph); 2.44 (2H; s; CH_2); 2.26 (3H; s; CH_3). ^{13}C NMR (75 MHz, Me_2SO): δ 163.2; 160.1; 159.8; 155.0; 154.9; 153.3; 150.4; 145.1; 140.8; 130.2; 122.2; 113.7; 112.9; 111.6; 111.6; 19.3. IR (KBr): ν_{max} 3350; 3063; 1718; 1693; 1607; 1557; 1276 cm^{-1}.

Calculation of Molecular Descriptors. Molecular models of the prepared aroylhydrazones were energy-minimized using a modified MM2 force field computation provided by ChemBio3D Ultra 11.0 (Cambridgesoft, Cambridge, MA, U.S.A.). From these models, various molecular descriptors were calculated. The logarithm of acid dissociation constant values (pK_a) was calculated using ACD/Laboratories Software V11.02 (Toronto, Canada).

HPLC Instruments and Methods. HPLC analyses were performed on a chromatographic system LC 20A Prominence (Shimadzu, Duisburg, Germany) consisting of a DGU-20A3 degasser, two LC-20 AD pumps, a SIL-20 AC autosampler, a CTO-20AC column oven, a PDA-detector, and a CBM-20AC communication module. The data were processed using LC solution software, version 1.21 SP1 (Shimadzu, Duisburg, Germany).

Table 1. Chromatographic Conditions Used in the Determination of the Stability of the New Chelators and SIH in Plasma[a]

	mobile phase composition				
chelator	pH of aqueous part[b]	organic part	ratio (v/v)	UV (nm)	I.S.
SIH	6	MeOH	53:47	288	*o*-108
HAPI	6	MeOH	55:45	288	*o*-108
HPPI	6	MeOH	60:40	288	*o*-108
2,4HAPI	6	MeOH	54:46	326	SIH
2,6HAPI	6	MeOH	55:45	300	*o*-108
MHAPI	6	MeOH/ACN[c]	50:50	328	SIH
CHAPI	6	MeOH/ACN[c]	40:60	285	SIH
NHAPI	3	MeOH	58:42	288	SIH
A2,4DHAPI	6	MeOH/ACN[c]	50:50	288	SIH
AHCI	6	MeOH	42:58	325	SIH

[a] I.S. = internal standard; ACN = acetonitrile; MeOH = methanol. [b] 10 mM Na_2HPO_4 and 2 mM EDTA. [c] A mixture of MeOH/ACN in a 1:1 ratio (v/v).

The analyses of the Fe chelators were performed on an analytical column (LiChrospher 250 mm × 4.6 mm, RP-18, 5 μm) protected with a guard column, both purchased from Merck (Darmstadt, Germany). The mobile phase was composed of a mixture of 10 mM phosphate buffer (with the addition of 2 mM EDTA) and either methanol or methanol/acetonitrile mixture in differing ratios. A flow rate of 1.0 mL/min, a column temperature of 25 °C, and an injection volume of 20 μL were used for the analysis. The quantification was made at the maximum absorption wavelength of the particular chelator. Either SIH or pyridoxal 2-chlorobenzoyl hydrazone (*o*-108) was used as the internal standard (I.S.). Detailed chromatographic conditions for each chelator are given in Table 1.

The linearity, precision, and accuracy of the methods were tested by the analysis of the sets of plasma samples spiked with different amounts of the chelators. Selectivity was confirmed by an analysis of blank plasma samples. All methods fulfilled the general validation criteria for bioanalytical methods.[32] SIH was analyzed using a previously developed and validated HPLC method.[27]

Assessments of Chelator Stabilities against Hydrolysis in Rabbit Plasma. The drug-free plasma was spiked with a standard solution of each chelator (1 mg/mL) to obtain a concentration of 100 μM. It was incubated in a water bath set at 37 ± 0.5 °C and mixed (120 rpm) during the entire experiment. At defined time intervals, 0.3 mL of plasma was transferred into Eppendorf tubes, and I.S. was added. The samples were treated by precipitation with acetonitrile (0.4 mL); the clear supernatant was injected onto the column. The stabilities of the chelators were determined as the percent decrease in the initial concentration with time.

Cell Culture. The H9c2 cell line, derived from embryonic rat heart tissue using selective serial passages,[33] was purchased from the American Type Culture Collection (Manassas, VA, U.S.A.; catalog # CRL-1446). Cells were cultured in Dulbecco's modified Eagle's medium (DMEM, Lonza, Belgium) supplemented with 10% heat inactivated fetal bovine serum (FBS, Lonza, Belgium), 1% penicillin/streptomycin solution (Lonza, Belgium), and 10 mM HEPES buffer (Sigma, Germany) in 75 cm^2 tissue culture flasks (TPP, Switzerland) at 37 °C in a humidified atmosphere of 5% CO_2. Subconfluent cells were subcultured every 3−4 days. For cytotoxicity experiments with neutral red (NR) as well as for experiments with acetoxymethyl ester of calcein green, cells were seeded in 96-well plates (TPP) at a density of 10,000 cells per well. For

morphological assessments, cells were seeded at a density of 75,000 cells per well in 12-well plates (TPP). Twenty-four hours prior to the experiments, the medium was changed to serum- and pyruvate-free DMEM (Sigma, Germany).

Determinations of Iron Chelating Efficiencies in Solution and Access to Cellular Labile Iron Pools. To assess the Fe chelation efficiencies of the newly synthesized agents in solution, measurements of calcein fluorescence intensity[34] were used. Calcein is a fluorescent probe readily forming complexes with Fe ions, which quench its fluorescence. Addition of Fe-chelating agent to the Fe-calcein leads to the removal of Fe from this complex with new complex formation. This is accompanied by an increase in fluorescence intensity.

The complex of calcein (free acid, 20 nM) with ferrous-diammonium sulfate (FAS; 200 nM) was prepared in HEPES buffered saline (150 mM NaCl and 40 mM HEPES; pH 7.2). Calcein and FAS were continuously stirred for 45 min in the dark after which >90% of fluorescence was quenched. Then 995 μL of the complex solution was pipetted into a stirred cuvette, and the baseline measurement was started. After 100 s, 5 μL of assessed potential Fe chelator solution was added yielding a final concentration of 5 μM. It should be noted, that as the ferrous ions (from FAS) get oxidized to ferric before the actual measurement, the assay is in effect looking at ferric iron binding.

The change in fluorescence intensity was measured as a function of time at 25 °C using a Perkin-Elmer LS50B fluorimeter (Perkin-Elmer, U. S.A.) at λ_{ex} = 486 nm and λ_{em} = 517 nm for 350 s. The Fe chelation efficiency in solution was expressed as a percentage of efficiency of the reference chelator SIH (100%).

The experiments analyzing iron chelating efficiencies in cultured cells were performed according to Glickstein et al.[35] with slight modifications. H9c2 cells were seeded on 96-well plates (10,000 cells per well). Twenty-four hours before the experiments, cells were loaded with 100 μM ferric-ammonium citrate (FAC) in serum-free medium. The cells were then washed and, to prevent potential interferences (especially with regard to various trace elements), the medium was replaced with a buffer prepared from Millipore-filtered (demineralized) water, containing 116 mM NaCl, 5.3 mM KCl, 1 mM $CaCl_2$, 1.2 mM $MgSO_4$, 1.13 mM NaH_2PO_4, 5 mM glucose, and 20 mM HEPES (pH 7.4). Cells were then loaded for 30 min at 37 °C with 1 μM cell-permeable acetoxymethyl ester of calcein green (Molecular Probes/KRD, Prague, Czech Republic) and washed. Cellular esterases cleave the acetoxymethyl groups to render the cell membrane-impermeable calcein green, whose fluorescence was quenched by FAC. Intracellular fluorescence (λ_{ex} = 488 nm; λ_{em} = 530 nm) was then followed in time (1 min before and 10 min after the addition of chelator) at 37 °C using an Infinite 200 M plate reader (Tecan, Austria).

Cytotoxicity Studies. Cellular viability was determined using a cytotoxicity assay based on the ability of viable cells to incorporate neutral red (NR). NR (Sigma, Germany) is a weak cationic dye that readily penetrates cell membranes by nonionic diffusion, accumulating intracellularly in lysosomes.[36] For vital stainings, after the experimental incubations, half the volume of medium from each well was removed, and the same volume of medium with NR was added (final concentration 40 μg/mL). After 3 h of incubation at 37 °C, the supernatant was discarded, and the cells were fixed in 0.5% formaldehyde with 1% $CaCl_2$ for 15 min, then were washed twice with PBS, and coagulated with 1% acetic acid in 50% ethanol, which released accumulated NR into the fluid where its optical density was measured at λ = 540 nm using a Tecan Infinite 200 M plate reader (Tecan, Austria). The viability of experimental groups was expressed as the percentage of untreated controls (100%).

Model oxidative injury was induced in H9c2 cells by their 24-h exposure to 200 μM *tert*-butyl hydroperoxide (*t*-BHP). The protective action of various iron chelators was assayed at different concentrations; chelators were added to cells 10 min before their exposure to *t*-BHP. In order to dissolve lipophilic chelators, Me_2SO (0.1% v/v) was present in the culture medium of all groups. At this concentration Me_2SO had no effect on cellular viability. Individual cytotoxicities of chelators were evaluated following 24 h and 72 h of incubations.

Changes in cellular morphology were evaluated using an epifluorescence inverted microscope Eclipse TS100 (Nikon, Japan) equipped with a digital cooled camera (1300Q, VDS Vosskühler, Germany) and software NIS-Elements AR 2.20 (Laboratory Imaging, Czech Republic). H9c2 cells were seeded on 12-well plates (75,000 cells per well) and incubated under conditions identical to those described above for NR uptake assays. Furthermore, cellular death was visualized using nuclei double staining with Hoechst 33342 and propidium iodide (PI; Molecular Probes) that are well established and sensitive procedures to determine apoptosis and necrosis.[14,16] Hoechst 33342 is a blue-fluorescent probe (λ_{ex}= 360 nm; λ_{em}= 460 nm) staining all nuclei. In apoptotic cells, chromatin condensation occurs, and apoptotic cells can thus be identified as those with condensed and more intensely stained chromatin. The red-fluorescent (λ_{ex} = 560 nm; λ_{em}= 630 nm) DNA-binding dye, PI, is unable to cross the plasma membrane of living cells but readily enters necrotic (or late-stage apoptotic) cells and stains their nuclei red. Cells were loaded with 10 μg/mL of Hoechst 33342 and 1 μg/mL of PI for 20 min at room temperature and sample images taken using the microscope setup described above.

Intracellular ROS Generation Measurements Using 2′,7′-Dichlorodihydrofluorescein-diacetate (H_2DCF-DA). The intracellular generation of ROS was assessed using the probe, 2′,7′-dichlorodihydrofluorescein-diacetate (H_2DCF-DA; Molecular Probes/KRD, Prague, Czech Republic). Cells were washed with buffer containing 116 mM NaCl, 5.3 mM KCl, 1 mM $CaCl_2$, 1.2 mM $MgSO_4$, 1.13 mM NaH_2PO_4, 5 mM glucose, and 20 mM HEPES (pH 7.4) and loaded with 10 μM H_2DCF-DA solution for 30 min at 37 °C. Cellular esterases cleave the acetyl groups to produce the cell membrane-impermeable compound H_2DCF, which becomes highly fluorescent when oxidized by ROS (particularly hydroxyl radicals and other highly oxidizing species) to DCF.[37] Following the addition of the tested substance(s), changes in intracellular fluorescence intensity (λ_{ex} = 488 nm; λ_{em} = 530 nm) were followed every 15 min for 1 h at 37 °C using the plate reader referenced above.

Data Analysis. The statistical software, SigmaStat for Windows 3.5 (SPSS, U.S.A.), was used in this study. Data are presented as the mean ± SE of a given number of experiments. Statistical significance was determined using Student's *t* test or ANOVA with a Bonferroni posthoc test (comparisons of multiple groups against a corresponding control). Data not displaying a normal distribution were evaluated using the nonparametric Mann−Whitney Rank Sum Test or Kruskal−Wallis ANOVA on Ranks with Dunn's test. Changes of chelator concentrations with time were evaluated with the Paired *t* test. Results were considered to be statistically significant when $p < 0.05$. The chelator concentration inducing 50% viability loss (TC_{50}) and the chelator concentration leading to 50% protection from *t*-BHP (EC_{50}) were calculated using CalcuSyn 2.0 software (Biosoft, Cambridge, U.K.). Pearson product−moment correlation analysis was used to determine dependences between various pairs of variables.

RESULTS

Stabilities of Chelators against Plasma Hydrolysis. Stabilities of the studied chelators in rabbit plasma *in vitro* were assessed by HPLC. The concentrations of the chelators were followed for 10 h, during which more than 50% degradation was observed for most of the compounds tested (Figure 2A−J). While the concentration of SIH decreased to 10% of its initial value already after 180 min of incubation, the novel analogues (except for 2,6DHAPI) were significantly more stable, with more

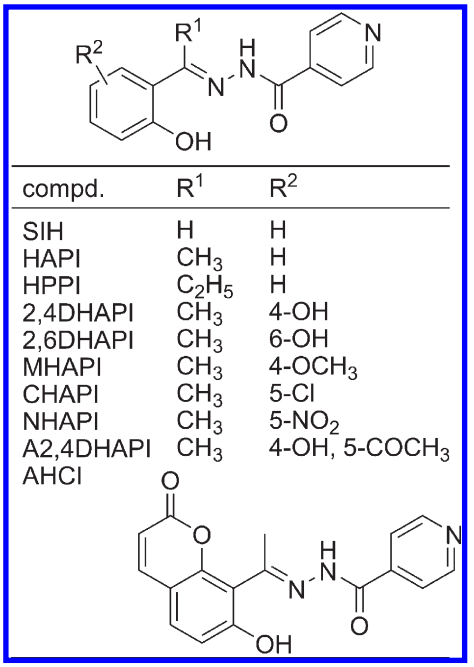

Figure 1. Chemical structures of SIH and the newly synthesized aroylhydrazone iron chelators.

than 50% of the initial concentrations still present at 180 min (Figure 2K). In the case of 2,6DHAPI, its concentration decreased to below the quantification limit of the HPLC method already at 360 min into the experiment. NHAPI was the most stable novel analogue, as less than 6% and 22% of its initial concentration underwent hydrolysis after 180 and 600 min, respectively. The sample chromatograms demonstrating the improved NHAPI stability in rabbit plasma in comparison with SIH are shown in Figure 3.

Iron-Chelating Efficiencies in Solution and Cell Culture. As seen in Figure 4A, all the nine newly synthesized aroylhydrazones showed high Fe-chelating activities in solution, which did not differ significantly from the reference chelator SIH. It should be noted though that at the 5 μM concentration the tested chelators were provided in large excess over calcein, and therefore this assay may have not discerned differences in their iron affinity.

In fact, diverse activities were detected with respect to the access to intracellular LIP in the H9c2 cardiomyoblast cell line. All the novel compounds displayed lower rates of intracellular calcein dequenching, and the unsubstituted ketone-derived analogues HAPI and HPPI were the only two agents which did not differ significantly from the parent chelator SIH (Figure 4B).

Protection from *tert*-Butyl Hydroperoxide-Induced Cellular Toxicity by Chelators. Incubation of H9c2 cells for 24 h with 200 μM *t*-BHP resulted in pronounced toxicity. Peripheral membrane blebbing was followed by the loss of spindle-like cell shape and rounding up of cells (Figure 5). Furthermore, severe nuclear condensation was conspicuous, and the nuclei were brightly stained with PI indicating cellular necrosis (or late-stage apoptosis). Complete loss of cellular viability was also clear from the NR uptake test (Figure 6). Co-treatment with either SIH or all of the newly synthesized Fe-chelating agents was able to preserve cellular morphology (Figure 5) as well as afford statistically significant increases in cellular viability (Figure 6), although at different concentrations. As compared to SIH, higher

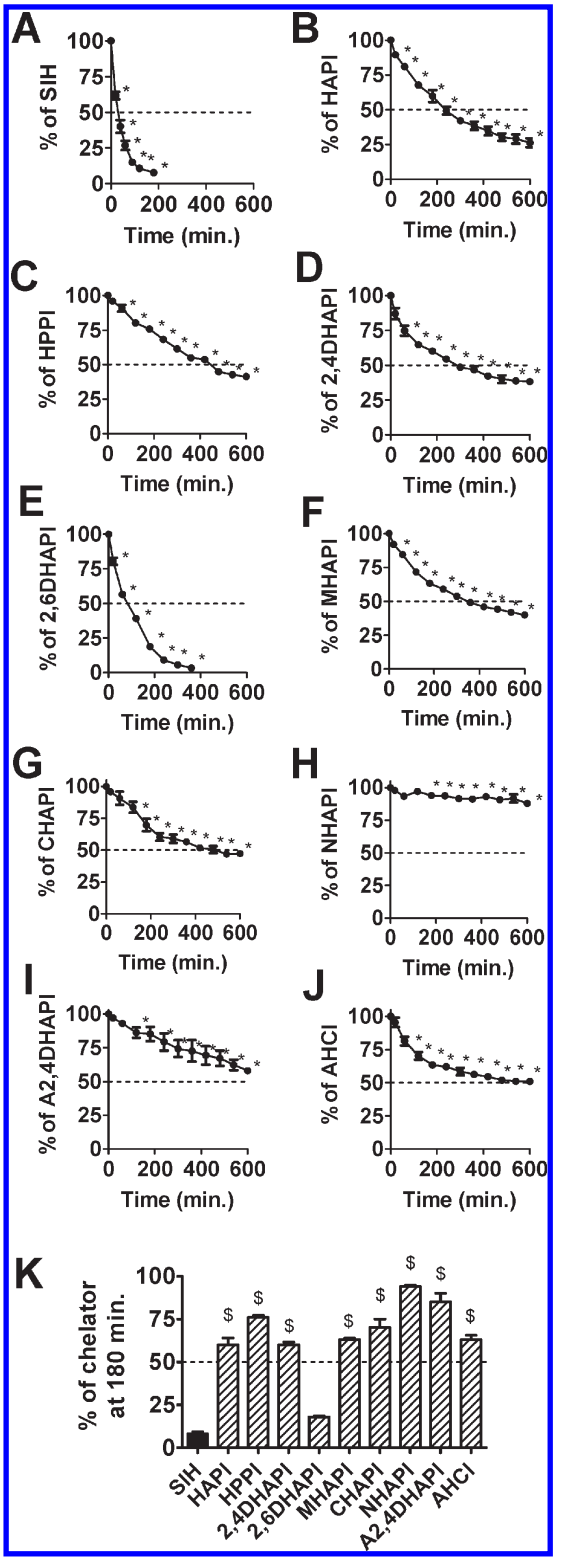

Figure 2. Stabilities of SIH and the new aroylhydrazone iron chelators in rabbit plasma. SIH (A), HAPI (B), HPPI (C), 2,4DHAPI (D), 2,6DHAPI (E), MHAPI (F), CHAPI (G), NHAPI (H), A2,4DHAPI (I), or AHCI (J) were incubated in rabbit plasma at 37 °C, and their concentration was followed in time using HPLC. Panel K shows the comparison of the remaining relative concentrations of the chelators following 180 min plasma incubations. Statistical significance: *, against initial concentration at $t = 0$ (paired t test; $p \leq 0.05$); $, comparison against SIH (ANOVA; $p \leq 0.05$).

dx.doi.org/10.1021/tx100359t |*Chem. Res. Toxicol.* 2011, 24, 290–302

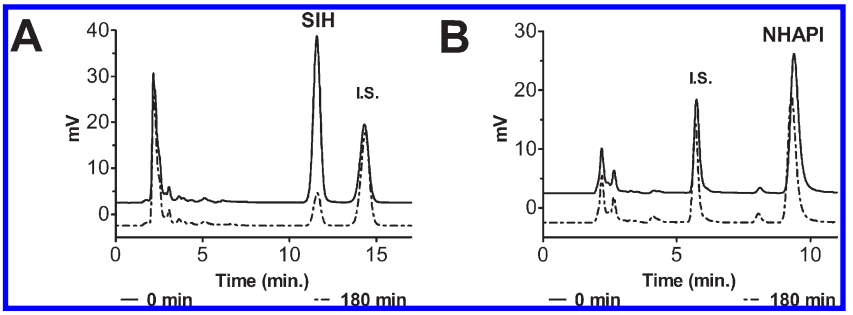

Figure 3. Sample chromatograms showing concentrations of chelators SIH (A) and NHAPI (B) in rabbit plasma at time 0 and following the 180 min incubations at 37 °C. I.S. = internal standard.

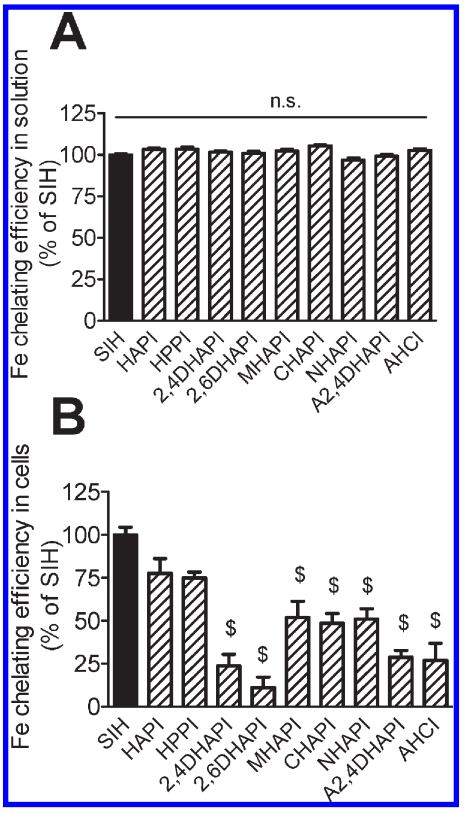

Figure 4. Iron chelation efficiencies of SIH, the newly synthesized agents and their access to cellular labile iron pool. (A) Displacement of iron from its complexes with calcein in buffered solution (pH 7.4) measured as an increase in fluorescence 10 min after the addition of chelator. (B) Displacement of intracellular labile iron from its complex with calcein in H9c2 cells 10 min after the addition of Fe chelators to extracellular medium. Iron chelating efficiencies are displayed as a percentage of SIH (100%). Results are presented as the mean ± SE (n = 4 experiments). Statistical significance (ANOVA; $p \leq 0.05$): $, compared to SIH.

protective efficiencies (resulting in lower EC_{50} values) were observed with HAPI, 2,4DHAPI, and CHAPI. In contrast, 2,6DHAPI, NHAPI, A2,4DHAPI, and AHCI had higher EC_{50} values as compared to those of SIH (Table 2). When compared at a single concentration (100 μM), which is the highest concentration at which most of the lipophilic agents (including SIH) could be dissolved, comparable protective actions of all of the chelators were observed, which did not differ significantly from those of SIH (Figure 7A).

Toxicities of Individual Chelators. In order to assess the cytotoxic effects of the tested chelators, we first incubated H9c2 cells with chelators for 24 h, i.e., the same time-period as that used for the cytoprotection experiments. All chelators were compared at 100 μM concentration, which is the solubility limit for most of them. As can be seen in Figure 7B, only SIH and CHAPI led to significant reduction of viability to approximately 55% of the control values. One hundred micromolar HAPI showed no sign of toxicity. Also with MHAPI, NHAPI, and A2,4DHAPI, the viability reduction ($\leq$15%) was insignificant as compared to the control and significantly less pronounced than that observed with SIH.

Given the marked differences in toxicities and limited solubility of the lipophilic agents, longer treatment periods were necessary to obtain TC_{50} values (i.e., chelator concentrations inducing 50% viability loss). Thus, the next set of experiments was performed with 72 h incubations. All chelators decreased cellular viability in a concentration-dependent manner; the results are shown in Figure 8, and the TC_{50} values summarized in Table 2. In addition, Figure 7C depicts a comparison of toxicities of all the chelators at 100 μM. NHAPI and AHCI were the least toxic agents; even incubations of cells with their 100 μM concentration did not induce a significant decrease in cell viability. In fact, their toxicities were very similar following the 24 and 72 h incubations. In all of the other agents, significant viability reduction below 50% occurred. The highest toxicities were observed with 2,4DHAPI, MHAPI, and CHAPI, with significantly lower viability observed from 3 μM concentrations.

Intracellular ROS Production. In the first set of experiments performed, intracellular ROS formation was induced by 200 μM t-BHP, and this resulted in a marked and statistically significant increase in intracellular H_2DCF oxidation (Figure 9A). With the exception of 2,4DHAPI, coincubations of t-BHP with all aroylhydrazone chelators resulted in a reduction in fluorescence intensity. SIH and MHAPI were the least effective agents, decreasing the rate of ROS formation only insignificantly, while 2,6DHAPI was the most potent, yielding a significant reduction of the fluorescence intensity comparable to that of the untreated control cells. Interestingly, 2,4DHAPI significantly augmented the t-BHP-induced ROS formation.

In the next series of studies, the cells were incubated for 60 min with the Fe donor, FAC (5 μM), either alone or in combination with the studied chelators (all at 10 μM concentrations, corresponding to the 1:2 Fe/chelator binding equivalent ratio). As demonstrated in Figure 9B, in cells incubated with FAC, the ROS production significantly increased as compared to that of the control. Coincubations with all chelators (except for 2,4DHAPI) resulted in reduction of the fluorescence intensity as compared to that of uncomplexed Fe, which reached statistical significance in the case of HAPI and 2,6DHAPI. Interestingly, incubation of cells with the Fe

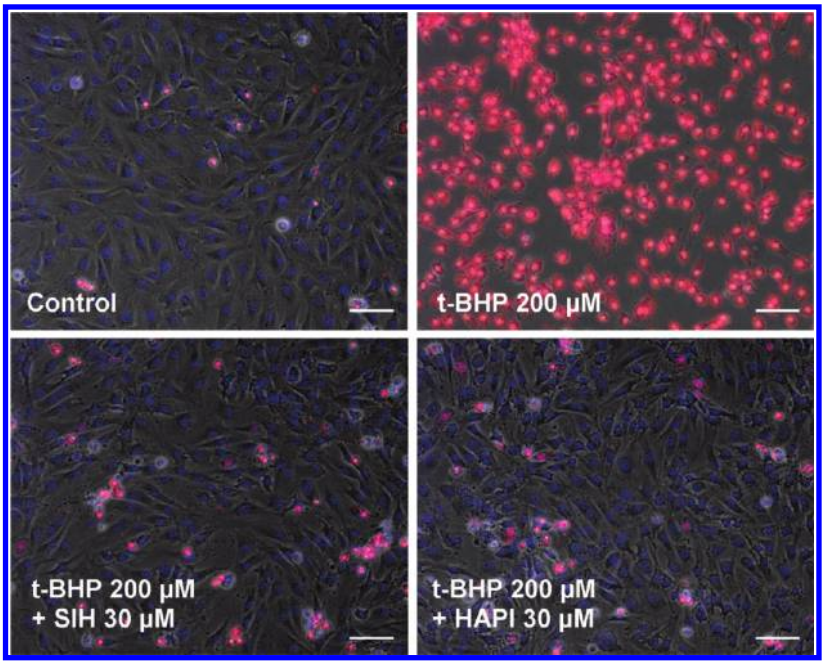

Figure 5. Cellular morphology and apoptosis/necrosis nuclear staining with Hoechst 33342 (blue) and propidium iodide (red) after a 24 h incubation of H9c2 cardiomyoblasts with 200 μM *tert*-butyl hydroperoxide and its combinations with iron chelators SIH and HAPI (both 30 μM). Scale bars 100 μm.

complexes of the two latter agents resulted in even lower levels of fluorescence than in control (Fe-free) cells (Figure 9B). Combination of FAC and 2,4DHAPI induced significant increase in cellular ROS levels.

In Figure 9C, the effects of chelators on spontaneous cellular ROS production are shown. 2,4DHAPI displayed a significant increase in DCF fluorescence as compared to both control and SIH-treated cells. All the other nine examined chelators did not significantly affect the spontaneous cellular ROS production.

Molecular Descriptors and Correlations. To obtain a basic insight into what molecular descriptors are important in interpreting the activity of the prepared compounds, correlation analyses were performed. Because of the small data set, no attempts at a detailed QSAR analysis were carried out; we only aimed at identifying any possible trends. All of the prepared aroylhydrazones comply with Lipinski's Rule of Five;[38] they have molecular weights from 241 to 323 g/mol, log *P* values of 1.4−3.1, up to 7 hydrogen bond acceptors, and up to 3 hydrogen bond donors. Both the ability of the compounds to protect the cells against the action of *t*-BHP and their toxicity significantly correlated with their polar surface area and pK_a of the phenolic hydroxyl (Figure 10). A significant relationship was also found between the protective efficacy of the compounds and their toxicity ($r = 0.88$, $r^2 = 0.78$,and $p < 0.001$). No significant correlations with other parameters were observed.

DISCUSSION

Aroylhydrazone Fe chelators represent an interesting group of biologically active molecules.[39] However, to date, these agents have not been thoroughly screened, and their structure−activity relationships were evaluated only for their ability to mobilize Fe from Fe overloaded cells[39,40] and their potential anticancer effects.[41] This study aimed at the assessment of their antioxidant properties against model oxidative injury of cardiomyoblast-derived cells induced by *t*-BHP. This organic peroxide is one of the most common membrane-permeable oxidant agents and has been used as a prototypic inducer of oxidative stress in numerous previous cellular experiments. Once inside cells, *t*-BHP generates *tert*-butoxy radicals, which induce various toxic effects including peroxidation of lipids, depletion of intracellular reduced glutathione, modification of protein thiols, or disturbance of calcium homeostasis.[1,42] *t*-BHP induces oxidative stress gradually over time and therefore induces sustained oxidative challenge to cells. Of note, *t*-BHP has been previously shown to release nonheme, nonferritin iron from rat liver microsomes.[43] Additional studies are nevertheless needed to examine the ROS formation and iron-mediated toxicity in cells exposed to stressors such as drugs that release iron from ferritin or heme sources.

The purpose of intracellular Fe chelation is to prevent redox-active Fe from engaging in radical-mediated cellular damage.[9,44,45] Previously, SIH has shown considerable potential in preventing various ROS-mediated pathologies both *in vitro* and *in vivo*. However, rapid plasma hydrolysis of SIH as well as other aldehyde-derived aroylhydrazones represents a serious obstacle to the effective *in vivo* application of these promising drug candidates.

Hence, the main purpose of our current study was to increase the chelator stability in plasma as compared to that of labile SIH while maintaining its favorable pharmacodynamic properties. The mechanism of the hydrolytic cleavage of the hydrazone bond involves protonation of the imine C═N nitrogen followed by a nucleophilic attack of water and cleavage of the C−N bond. Therefore, our first hypothesis was that the replacement of the aldimine hydrogen in SIH by a bulkier and electron-donating alkyl group would decrease the probability of attack of water on the C═N carbon and thus improve the compound stability. This was indeed confirmed; both methylketone-derived HAPI and ethylketone-derived HPPI were shown as significantly more stable and resistant against hydrolysis in plasma than SIH.

The second approach was to modify the substituents on the phenyl ring to investigate their effects on the hydrazone bond stability. The literature reports, particularly on this issue, were somewhat contradictory. For example, replacement of pyridine

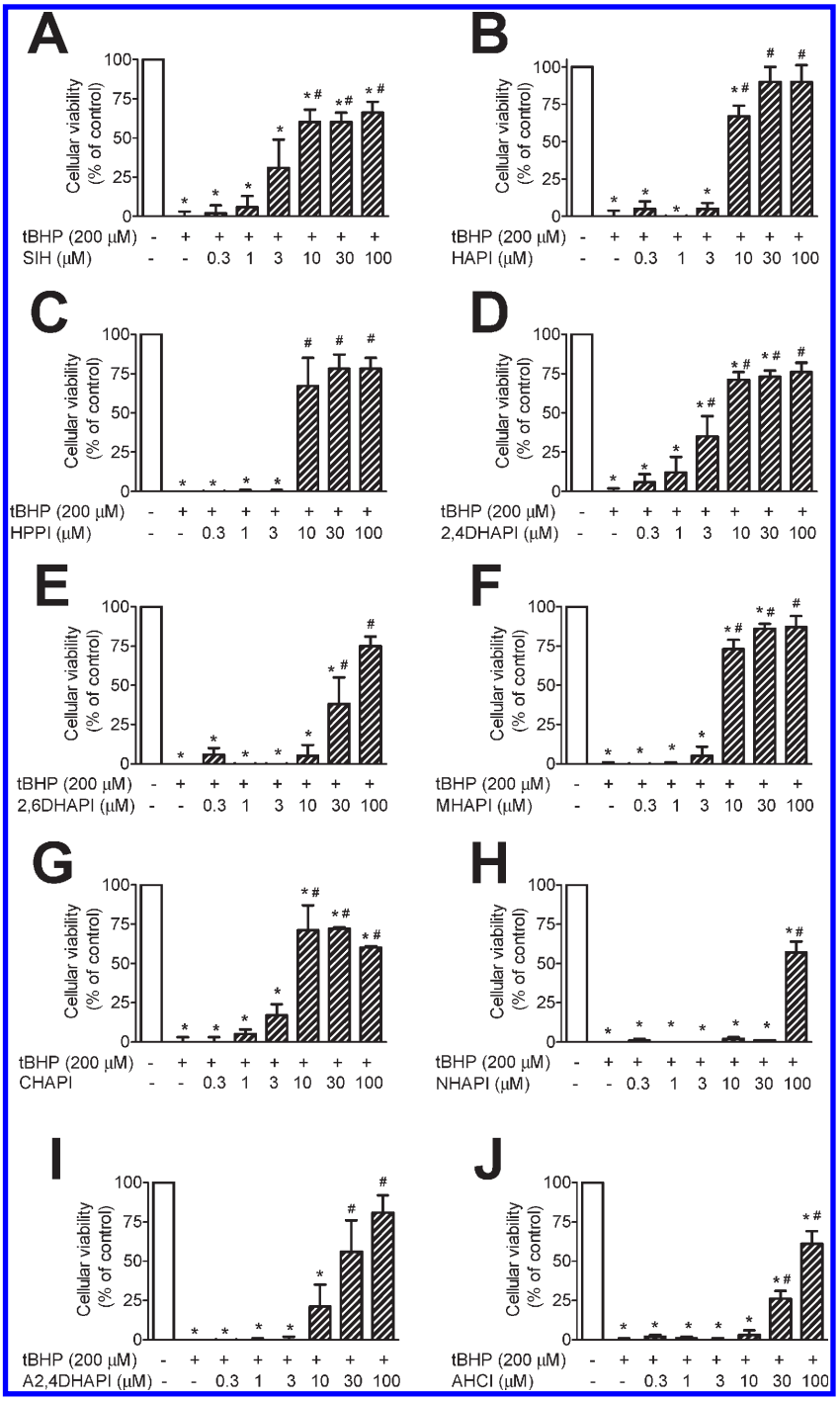

Figure 6. Effects of various concentrations of iron chelators SIH (A), HAPI (B), HPPI (C), 2,4DHAPI (D), 2,6DHAPI (E), MHAPI (F), CHAPI (G), NHAPI (H), A2,4DHAPI (I), or AHCI (J) on cellular toxicity induced in H9c2 cells by a 24 h incubation with 200 μM *tert*-butyl hydroperoxide (*t*-BHP). Studies were performed using the neutral red uptake test, and the results are presented as mean ± SE ($n \geq 4$ experiments). Statistical significance (ANOVA; $p \leq 0.05$): *, compared to the control (untreated) group; #, compared to the 200 μM *t*-BHP group.

in SIH (and also in PIH) by a phenyl ring markedly increased their hydrolytic stability.[46] This was explained by an increased electron density at the hydrazone C═N carbon and, consequently, its lower susceptibility to the attack of water after the removal of the strong electron-withdrawing nitrogen. This seems to be in contrast with our results; however, it should be noted that the aforementioned structural alterations[46] were on the other side of the hydrazone bond and might have influenced the distribution of the electron density on the hydrazone C═N bond differently. Nevertheless, compound NHAPI, containing the strongest electron acceptor of all the novel chelators, was the most stable compound in our study. This effect was consistently found in all of the studied hydrazones containing electron-withdrawing groups, i.e., acetyl in A2,4DHAPI increased its stability compared to that of 2,4DHAPI, and CHAPI bearing chlorine in position 5 was more stable than HAPI, while those

dx.doi.org/10.1021/tx100359t |*Chem. Res. Toxicol.* 2011, 24, 290–302

Table 2. Selected Characteristics of the Evaluated Iron Chelators[a]

chelator	MW (g/mol)	log *P*	PSA (Å^2)	pK_a	EC_{50} (μM)	TC_{50} (μM)
SIH	241	2.1	75	8.5	18.2	29.7
HAPI	255	2.1	75	8.5	11.4	12.2
HPPI	269	2.6	75	8.5	17.8	29.2
2,4DHAPI	271	1.4	95	8.2	9.2	2.7
2,6DHAPI	271	1.4	95	7.6	48.3	31.2
MHAPI	285	2.2	84	7.8	21.2	9.5
CHAPI	290	3.1	75	8.0	9.5	4.8
NHAPI	300	2.5	121	5.6	68.5	>100[b]
A2,4DHAPI	313	2.0	112	7.2	39.9	73.3
AHCI	323	2.2	100	6.3	56.6	>100[b]

[a] MW, molecular weight; log *P*, logarithm of octanol/water partition coefficient; PSA, polar surface area calculated using ChemBioOffice Ultra 11.0 (Cambridgesoft, Cambridge, MA); pK_a, logarithm of acid dissociation constant of the phenolic hydroxyl calculated using ACD/Labs Software V11.02 (Toronto, Canada); EC_{50}, concentration of chelator reducing the toxicity induced by 24-h incubation with *tert*-butyl hydroperoxide to 50% of the control (untreated) cells; TC_{50}, chelator concentration inducing 50% viability reduction compared to control (untreated) cells following 72 h incubation. Neutral red uptake assay; mean values of $n \geq 4$ experiments. [b] Exceeds solubility limit.

with electron donors displayed stability similar to that of unsubstituted HAPI. A possible explanation of these results is that electron acceptors decrease the electron density on C=N nitrogen and decrease its protonation, which is consistent with a previous study on hydrazone basicity.[47] Thus, protonation of the C=N nitrogen seems to be the key factor in the hydrolysis of the methylketone-based hydrazones. It should be noted that the effects of certain substituents on hydrazone stability also depend on pH; for example, the nitro group increased the hydrazone hydrolysis rate at lower pH but decreased it in a neutral or basic environment.[48] Interestingly, it was found that 2,6DHAPI was much less stable compared to its position isomer 2,4DHAPI. This observation could be explained by the steric effect of hydroxyls in both *o*-positions. In general, aromatic hydrazones are more stable to acidic hydrolysis than the aliphatic ones due to a conjugation of the π electrons of the C=N bond with the aromatic ring.[49] However, such conjugation requires coplanarity of the aromatic ring with the C=N bond, which may be hindered by repulsion between the methyl group and one of the *o*-hydroxyls.

The marked improvement in plasma stability of the ketone-derived SIH analogues is an important, but by no means sufficient, outcome of this study. The newly synthesized analogues had to retain their Fe-chelating, antioxidant, and cytoprotective activities as well as possess acceptable specific toxicity. As all of the three structural moieties of SIH responsible for Fe binding remained unchanged, all these agents displayed expectably high Fe-chelating activity in solution, comparable to that of SIH. However, in terms of access to intracellular LIP, the new chelators displayed lower efficiencies as compared to that of SIH. The decrease in the chelation of intracellular free Fe was significant in all the agents except for the unsubstituted HAPI and HPPI. The lowest access to cellular Fe was observed in 2,4DHAPI and 2,6DHAPI. In contrast, most of the new agents were shown to block intracellular ROS production more efficiently than SIH. Interestingly, the highest antioxidant action was

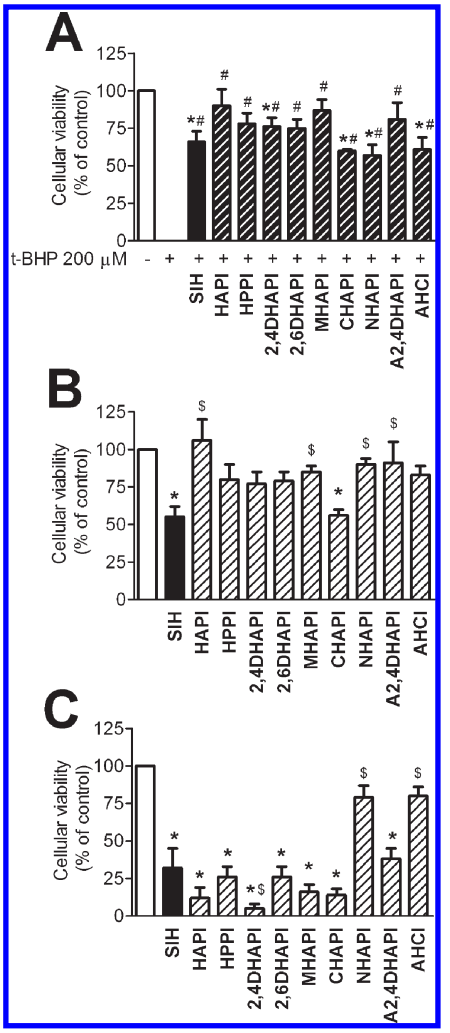

Figure 7. (A) Protective effects of various aroylhydrazone iron chelators (100 μM) against cellular injury induced to H9c2 cells by a 24 h incubation with *tert*-butyl hydroperoxide (*t*-BHP; 200 μM). (B) Effects of a 24 h incubation with these chelators at 100 μM concentration on cellular viability. (C) Effects of a 72 h incubation with these chelators at 100 μM concentration on cellular viability. Studies were performed using the neutral red uptake test, and the results are presented as mean ± SE ($n \geq 4$ experiments). Statistical significance (ANOVA; $p \leq 0.05$): *, compared to the control (untreated) group; #, compared to the 200 μM *t*-BHP group; $, compared to the SIH group.

observed with 2,6DHAPI, whereas its position isomer 2,4DHAPI displayed a totally opposite effect: it rather augmented the cellular ROS burst. It should be noted that the higher increase in ROS production was observed when the cells were incubated with 2,4DHAPI alone (Figure 8C) than with the 2,4DHAPI-Fe combination (Figure 8B), suggesting that this agent may promote ROS formation per se, rather than by forming a redox-active Fe complex. Interestingly, this pro-oxidant property of 2,4DHAPI was not shared by either its position isomer 2,6DHAPI or A2,4DHAPI, which contains an additional acetyl in position 5 compared to 2,4DHAPI. This may be because the hydroxyl in position 4 together with free positions 3 and 5 of the phenyl ring of 2,4DHAPI may resemble the phenol-type substitution pattern in the B ring of flavonoids such as apigenin, naringenin, or naringin, which act as pro-oxidants without involving a transition metal-catalyzed autoxidation.[50]

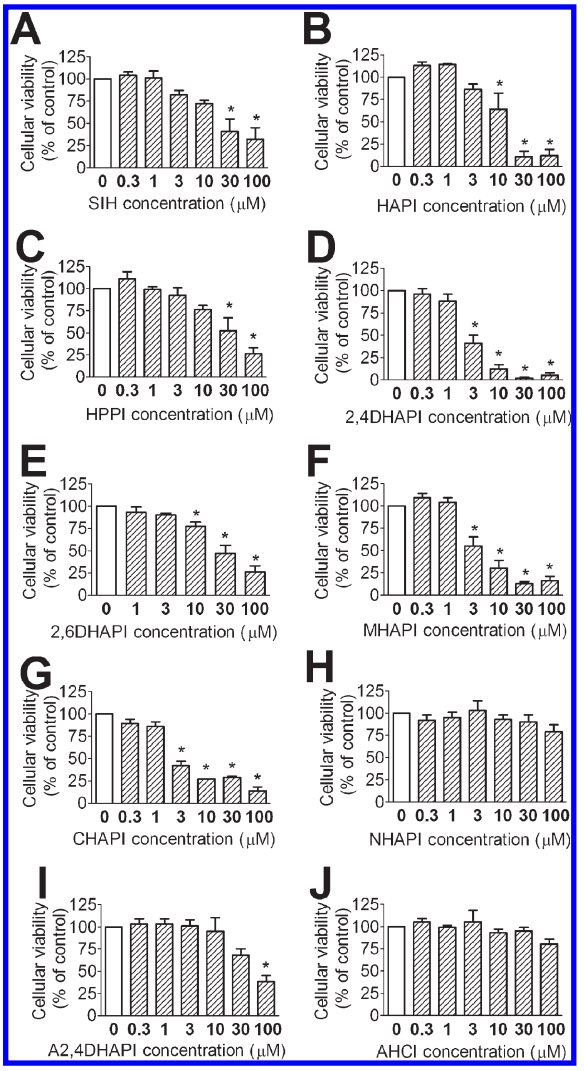

Figure 8. Effects of a 72 h incubation with iron chelators SIH (A), HAPI (B), HPPI (C), 2,4DHAPI (D), 2,6DHAPI (E), MHAPI (F), CHAPI (G), NHAPI (H), A2,4DHAPI (I), or AHCI (J) on the cellular viability of H9c2 cells. Studies were performed using the neutral red uptake, and the results are presented as the mean ± SE ($n \geq 4$ experiments). Statistical significance (ANOVA; $p \leq 0.05$): *, compared to the control (untreated) group.

Despite all of the differences discussed above, all of these agents were able to protect the cells against the model oxidative injury induced by *t*-BHP, although with variable efficiencies. Notably, the protective efficiencies of the studied hydrazones (expressed as the EC_{50} values) correlated with their molecular polar surface area. This value is defined as the sum of the surface areas of polar atoms and serves as a useful parameter for the prediction of passive transport through cellular membranes.[51,52] All of the studied compounds have polar surface area values from 75 to 121 $Å^2$, which is within the limit of 140 $Å^2$ for penetrating cell membranes.[53] Thus, we suppose that the observed changes in protective efficiencies and toxicities of the studied compounds compared to SIH are related to their different abilities to penetrate into the cells. Of note, it is commonly assumed that such correlations are sigmoidal. However, in this study, linear relationships were observed. This may be explained by two factors: first, the compounds are structurally related, and second,

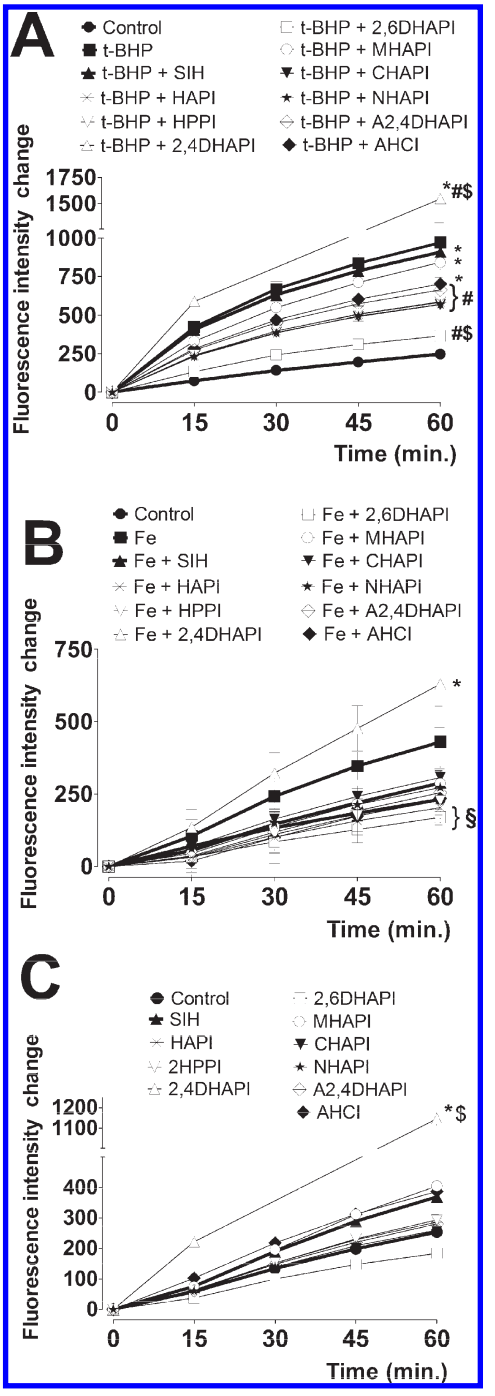

Figure 9. Intracellular reactive oxygen species production in H9c2 cells loaded with H_2DCF-DA (diacetate ester of reduced 2′,7′-dichlorofluorescein) and exposed for 60 min to *tert*-butyl hydroperoxide (*t*-BHP), ferric ammonium citrate (FAC), and/or various aroylhydrazone Fe chelators. Following intracellular acetate group cleavage, the increase in fluorescence intensity (λ_{ex} = 488; λ_{em} = 520 nm) is proportional to probe oxidation by reactive oxygen species to green fluorescent DCF. (A) Effects of chelators on an oxidative burst induced by incubation with 200 μM *t*-BHP; (B) effects of iron chelators on probe oxidation induced by incubation with 5 μM FAC; (C) effects of Fe chelators alone (all 10 μM). Results are presented as the mean ± SE (n = 4 experiments). Statistical significance (ANOVA; $p \leq 0.05$): *, compared to the control (spontaneous H_2DCF oxidation); #, compared to the *t*-BHP group; §, compared to the FAC group; $, compared to the SIH group.

dx.doi.org/10.1021/tx100359t |*Chem. Res. Toxicol.* 2011, 24, 290–302

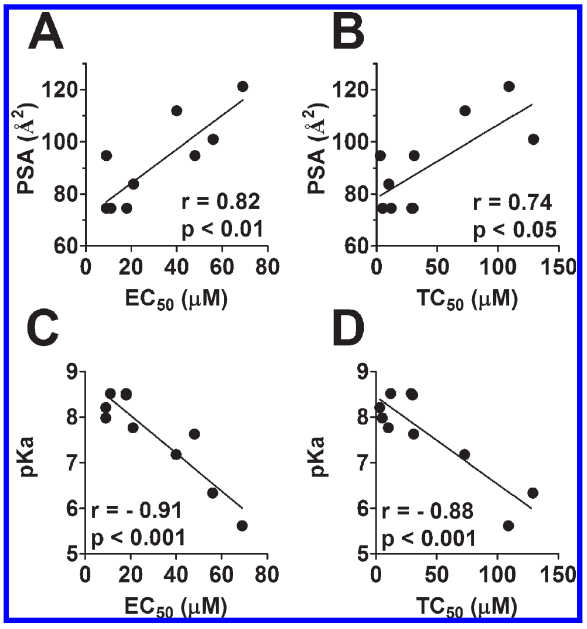

Figure 10. Scatterplots and correlations between protective efficiencies (EDC_{50} values, panels A and C) and long-term toxicities (TC_{50} values, panels B and D), and the molecular parameters of the studied aroylhydrazones including polar surface area (PSA, panels A and B) and acidity of the phenolic hydroxyl (pK_a, panels C and D). *r*, Pearson product−moment correlation coefficients; *p*, statistical significance of the correlation.

they possess medium polar surface area values, which would be located at the central linear part of the sigmoidal curve.

The assumption that the ability of the studied aroylhydrazones to protect cells against the action of *t*-BHP is related to their penetration through the cell membrane is further supported by the strong correlation observed between this ability and the pK_a of the phenolic hydroxyl. Since pK_a values range from 5.6 to 8.5, the ratio of negatively charged/neutral molecules will be starkly different at physiological pH 7.4. For example, introduction of a nitro group in NHAPI resulted in a markedly increased acidity of the phenolic hydroxyl compared to that of HAPI due to the strongly electron-withdrawing properties of the nitro group. Thus, this compound is ∼99% ionized at pH 7.4 and cannot be expected to penetrate the lipophilic cell membrane readily, which is in agreement with its low protective effect. These pronounced differences in ionization at around pH 7.4 may also explain the lack of correlation of the protective activities and/or toxicities of the chelators with their log *P*.

In order to fully assess the therapeutic potential of these new aroylhydrazones, it was also necessary to determine their own individual toxicities. It is known that the use of Fe chelators in states without Fe overload is associated with the obvious risk of toxicity due to the removing or withholding of Fe from critical Fe-containing proteins and/or the interaction with normal Fe metabolism. On the one hand, the low stability of SIH and other aldehyde-derived aroylhydrazones may have led to the underestimation of the pharmacological potential of these chelators in previous studies. However, on the other hand, the desired increase in stability may also potentiate the risk of the toxicity of these new chelators, especially in long-term treatment.[9] In fact, improved hydrolytic stability is an important feature of novel cytotoxic thiosemicarbazone Fe chelators, which are currently studied for the treatment of cancer.[54,55]

In this study, the individual toxicities of the tested compounds toward H9c2 cells were determined following 24- and 72-h incubations. Interestingly, with the exception of CHAPI, the increase in chelator stability resulted in the decrease of their toxicity following the 24-h cellular treatments as compared to SIH. This may be related to the lower release of toxic isoniazid by the new chelators, as compared to labile SIH. In contrast, following the long (72 h) incubations, enhancement in the toxicities occurred in most of the agents, except for AHCI and NHAPI. The highest inherent long-term toxicity (the lowest TC_{50}) as well as the worst ratio of protective efficiency and own toxicity (EC_{50}/TC_{50}) was observed with 2,4DHAPI, which may be caused by its pro-oxidant properties. Indeed, some of the aroylhydrazone chelators may, apart from Fe deprivation, induce toxicity due to oxidative stress induction.[56] Nevertheless, as shown by the DCF assay, other studied agents seem unlikely to act as pro-oxidants.

In some agents, a certain discrepancy has been observed between the results of cytoprotection experiments against *t*-BPH toxicity and the experiments where the intracellular ROS formation was evaluated using the H_2DCF-DA assay. For instance, SIH was very effective in protecting the cells according to the first experiment (Figure 6A), but the results from the second one seem to suggest that it does not have a significant effect on ROS generation (Figure 9A). It is possible that apart from forming the alkoxyl radicals *t*-BHP may activate various peroxidases to compound I or II[1] that eventually oxidize H_2DCF to DCF, and the various chelating agents may affect DCF levels by interfering with the catalytic cycle of peroxidases.

In conclusion, all of the newly synthesized SIH analogues were shown as significantly more resistant against the hydrazone bond hydrolysis, with the exception of 2,6DHAPI. At the same time, these agents retained their ability to protect the cardiac-derived cells against Fe-mediated oxidative injury. In particular, the novel chelator HAPI shows promise due to the absence of short-term toxicity and improved antioxidant and cytoprotective action with preserved access to LIP as compared to the reference chelator SIH. HAPI might be especially useful in acute situations, e.g., for short periods of treatment during which temporary Fe deprivation could be tolerable, such as in ischemia/reperfusion injury.

On the other hand, due to its negligible long-term toxicity and high plasma stability, NHAPI may be beneficial in animal experiments requiring long-term chelator exposure, such as in studies on atherosclerosis or heart failure. Further detailed studies are necessary to confirm the cardioprotective efficacies and toxicities of these novel drug candidates using more complex *in vivo* models, as well as to determine their potential clinical implications.

AUTHOR INFORMATION

Corresponding Author

*(K.V.) Department of Inorganic and Organic Chemistry, Charles University in Prague, Faculty of Pharmacy, Heyrovskeho 1203, 500 05 Hradec Kralove, Czech Republic. Tel: +420-495-067-497. Fax: +420-495-067-166. E-mail: Katerina.Vavrova@faf.cuni.cz. (T.S.) Department of Biochemical Sciences, Charles University in Prague, Faculty of Pharmacy, Heyrovskeho 1203, 500 05 Hradec Kralove, Czech Republic. Tel: +420-495-067-422. Fax: +420-495-067-168. E-mail: Tomas.Simunek@faf.cuni.cz.

Funding Sources

This study was supported by the Charles University in Prague (grants SVV 2010/261/001 and 2010/261/003) and Ministry of Education of the Czech Republic (Research Project MSM0021620822).

■ ACKNOWLEDGMENT

We thank Mrs. Alena Pakostova for her technical assistance in the cell-culture laboratory.

■ ABBREVIATIONS

A2,4DHAPI, (*E*)-*N*′-[1-(5-acetyl-2,4-dixydroxyphenyl)ethyliden]-isonicotinoylhydrazide; AHCI, (*E*)-*N*′-(1-(7-hydroxy-2-oxo-2*H*-chromen-8-yl)ethylidene)isonicotinohydrazide; CHAPI, (*E*)-*N*′-[1-(5-chloro-2-hydroxyphenyl)ethyliden]isonicotinoylhydrazide; DCF, dichlorofluorescein; DFO, desferioxamine; 2,4DHAPI, (*E*)-*N*′-[1-(2,4-dihydroxyphenyl)ethyliden]isonicotinoylhydrazide; 2,6-DHAPI, (*E*)-*N*′-[1-(2,6-dihydroxyphenyl)ethyliden]isonicotinoylhydrazide; DMEM, Dulbecco's modified Eagle's medium; EC_{50}, concentration of chelator reducing the toxicity induced by 24-h incubation with *tert*-butyl hydroperoxide to 50% of the control (untreated) cells; FAC, ferric-ammonium citrate; FAS, ferrous-diammonium sulfate; FBS, fetal bovine serum; Fe, iron; HAPI, (*E*)-*N*′-[1-(2-hydroxyphenyl)ethyliden]isonicotinoylhydrazide; H_2DCF-DA, 2′,7′-dichlorodihydrofluorescein-diacetate; HPPI, (*E*)-*N*′-[1-(2-hydroxyphenyl)propyliden]isonicotinoylhydrazide; ICL670A, deferasirox; ICRF-187, dexrazoxane; I.S., internal standard; L1 or CP20, deferiprone; LIP, labile iron pool; log *P*, logarithm of octanol/water partition coefficient; MHAPI, (*E*)-*N*′-[1-(2-hydroxy-4-methoxyphenyl)-ethyliden]isonicotinoylhydrazide; MW, molecular weight; NHAPI, (*E*)-*N*′-[1-(2-hydroxy-5-nitrophenyl)ethyliden]isonicotinoylhydrazide; NR, neutral red; PI, propidium iodide; PSA, polar surface area; QSAR, quantitative structure−activity relationship; ROS, reactive oxygen species; RT, room temperature; SIH, salicylaldehyde isonicotinoyl hydrazone; *t*-BHP, *tert*-butyl hydroperoxide; TC_{50}, concentration of the chelator inducing 50% viability reduction compared to the control (untreated) cells following 72 h of incubation.

■ REFERENCES

(1) Halliwell, B., and Gutteridge, J. M. C. (2007) *Free Radicals in Biology and Medicine*, 4th ed., Oxford University Press, Oxford, U.K.

(2) Griendling, K. K., and FitzGerald, G. A. (2003) Oxidative stress and cardiovascular injury: Part I: basic mechanisms and in vivo monitoring of ROS. *Circulation 108*, 1912–1916.

(3) Simunek, T., Sterba, M., Popelova, O., Adamcova, M., Hrdina, R., and Gersl, V. (2009) Anthracycline-induced cardiotoxicity: overview of studies examining the roles of oxidative stress and free cellular iron. *Pharmacol. Rep. 61*, 154–171.

(4) Mladenka, P., Simunek, T., Hubl, M., and Hrdina, R. (2006) The role of reactive oxygen and nitrogen species in cellular iron metabolism. *Free Radical Res. 40*, 263–272.

(5) Reif, D. W. (1992) Ferritin as a source of iron for oxidative damage. *Free Radical Biol. Med. 12*, 417–427.

(6) Kalinowski, D. S., and Richardson, D. R. (2005) The evolution of iron chelators for the treatment of iron overload disease and cancer. *Pharmacol. Rev. 57*, 547–583.

(7) Olivieri, N. F., and Brittenham, G. M. (1997) Iron-chelating therapy and the treatment of thalassemia. *Blood 89*, 739–761.

(8) Wood, J. C. (2008) Cardiac iron across different transfusion-dependent diseases. *Blood Rev. 22* (Suppl. 2), S14–S21.

(9) Galey, J. B. (2001) Recent advances in the design of iron chelators against oxidative damage. *Mini Rev. Med. Chem. 1*, 233–242.

(10) Hasinoff, B. B., Hellmann, K., Herman, E. H., and Ferrans, V. J. (1998) Chemical, biological and clinical aspects of dexrazoxane and other bisdioxopiperazines. *Curr. Med. Chem. 5*, 1–28.

(11) Horackova, M., Ponka, P., and Byczko, Z. (2000) The antioxidant effects of a novel iron chelator salicylaldehyde isonicotinoyl hydrazone in the prevention of H(2)O(2) injury in adult cardiomyocytes. *Cardiovasc. Res. 47*, 529–536.

(12) Kurz, T., Gustafsson, B., and Brunk, U. T. (2006) Intralysosomal iron chelation protects against oxidative stress-induced cellular damage. *FEBS J. 273*, 3106–3117.

(13) Lukinova, N., Iacovelli, J., Dentchev, T., Wolkow, N., Hunter, A., Amado, D., Ying, G. S., Sparrow, J. R., and Dunaief, J. L. (2009) Iron chelation protects the retinal pigment epithelial cell line ARPE-19 against cell death triggered by diverse stimuli. *Invest. Ophthalmol. Vis. Sci. 50*, 1440–1447.

(14) Simunek, T., Boer, C., Bouwman, R. A., Vlasblom, R., Versteilen, A. M., Sterba, M., Gersl, V., Hrdina, R., Ponka, P., de Lange, J. J., Paulus, W. J., and Musters, R. J. (2005) SIH: a novel lipophilic iron chelator--protects H9c2 cardiomyoblasts from oxidative stress-induced mitochondrial injury and cell death. *J. Mol. Cell Cardiol. 39*, 345–354.

(15) Bendova, P., Mackova, E., Haskova, P., Vavrova, A., Jirkovsky, E., Sterba, M., Popelova, O., Kalinowski, D. S., Kovarikova, P., Vavrova, K., Richardson, D. R., and Simunek, T. (2010) Comparison of clinically used and experimental iron chelators for protection against oxidative stress-induced cellular injury. *Chem. Res. Toxicol. 23*, 1105–1114.

(16) Simunek, T., Sterba, M., Popelova, O., Kaiserova, H., Adamcova, M., Hroch, M., Haskova, P., Ponka, P., and Gersl, V. (2008) Anthracycline toxicity to cardiomyocytes or cancer cells is differently affected by iron chelation with salicylaldehyde isonicotinoyl hydrazone. *Br. J. Pharmacol. 155*, 138–148.

(17) Sterba, M., Popelova, O., Simunek, T., Mazurova, Y., Potacova, A., Adamcova, M., Guncova, I., Kaiserova, H., Palicka, V., Ponka, P., and Gersl, V. (2007) Iron chelation-afforded cardioprotection against chronic anthracycline cardiotoxicity: a study of salicylaldehyde isonicotinoyl hydrazone (SIH). *Toxicology 235*, 150–166.

(18) Berndt, C., Kurz, T., Selenius, M., Fernandes, A. P., Edgren, M. R., and Brunk, U. T. (2010) Chelation of lysosomal iron protects against ionizing irradiation. *Biochem. J. 432*, 295–301.

(19) Klimtova, I., Simunek, T., Mazurova, Y., Kaplanova, J., Sterba, M., Hrdina, R., Gersl, V., Adamcova, M., and Ponka, P. (2003) A study of potential toxic effects after repeated 10-week administration of a new iron chelator--salicylaldehyde isonicotinoyl hydrazone (SIH) to rabbits. *Acta Med. (Hradec Kralove, Czech Repub.) 46*, 163–170.

(20) Yiakouvaki, A., Savovic, J., Al-Qenaei, A., Dowden, J., and Pourzand, C. (2006) Caged-iron chelators a novel approach towards protecting skin cells against UVA-induced necrotic cell death. *J. Invest. Dermatol. 126*, 2287–2295.

(21) Charkoudian, L. K., Dentchev, T., Lukinova, N., Wolkow, N., Dunaief, J. L., and Franz, K. J. (2008) Iron prochelator BSIH protects retinal pigment epithelial cells against cell death induced by hydrogen peroxide. *J. Inorg. Biochem. 102*, 2130–2135.

(22) Charkoudian, L. K., Pham, D. M., and Franz, K. J. (2006) A prochelator triggered by hydrogen peroxide inhibits iron-promoted hydroxyl radical formation. *J. Am. Chem. Soc. 128*, 12424–12425.

(23) Kovarikova, P., Klimes, J., Sterba, M., Popelova, O., Mokry, M., Gersl, V., and Ponka, P. (2005) Development of high-performance liquid chromatographic determination of salicylaldehyde isonicotinoyl hydrazone in rabbit plasma and application of this method to an in vivo study. *J. Sep. Sci. 28*, 1300–1306.

(24) Buss, J. L., and Ponka, P. (2003) Hydrolysis of pyridoxal isonicotinoyl hydrazone and its analogs. *Biochim. Biophys. Acta 1619*, 177–186.

(25) Richardson, D., Vitolo, L. W., Baker, E., and Webb, J. (1989) Pyridoxal isonicotinoyl hydrazone and analogues. Study of their stability in acidic, neutral and basic aqueous solutions by ultraviolet-visible spectrophotometry. *BioMetals 2*, 69–76.

(26) Kovarikova, P., Mokry, M., Klimes, J., and Vavrova, K. (2006) HPLC study on stability of pyridoxal isonicotinoyl hydrazone. *J. Pharm. Biomed. Anal. 40*, 105–112.

(27) Kovarikova, P., Mrkvickova, Z., and Klimes, J. (2008) Investigation of the stability of aromatic hydrazones in plasma and related biological material. *J. Pharm. Biomed. Anal. 47*, 360–370.

(28) Simunek, T., Sterba, M., Popelova, O., Kaiserova, H., Potacova, A., Adamcova, M., Mazurova, Y., Ponka, P., and Gersl, V. (2008) Pyridoxal isonicotinoyl hydrazone (PIH) and its analogs as protectants against anthracycline-induced cardiotoxicity. *Hemoglobin 32*, 207–215.

(29) Edward, J. T., Gauthier, M., Chubb, F. L., and Ponka, P. (1988) Synthesis of new acylhydrazones as iron-chelating compounds. *J. Chem. Eng. Data 33*, 538–540.

(30) Sacconi, L. (1953) Acylhydrazones of ortho-oxyaldehydes and ortho-aminoaldehydes and ketones as tridentate complexing agents. *J. Am. Chem. Soc. 75*, 5434–5435.

(31) Kumar, S., and Kumar, D. (2008) Polystyrene-supported iodobenzene diacetate (PSIBD)-mediated synthesis of 1,2-diacylbenzenes from 2-hydroxyaryl aldehyde/ketone acylhydrazones. *Synth. Commun. 38*, 3683–3699.

(32) FDA *Guidance for Industry: Bioanalytical Method Validation*, May 2001, http://www.fda.gov/downloads/Drugs/GuidanceComplianceRegulatoryInformation/Guidances/UCM070107.pdf.

(33) Kimes, B. W., and Brandt, B. L. (1976) Properties of a clonal muscle cell line from rat heart. *Exp. Cell Res. 98*, 367–381.

(34) Esposito, B. P., Epsztejn, S., Breuer, W., and Cabantchik, Z. I. (2002) A review of fluorescence methods for assessing labile iron in cells and biological fluids. *Anal. Biochem. 304*, 1–18.

(35) Glickstein, H., El, R. B., Link, G., Breuer, W., Konijn, A. M., Hershko, C., Nick, H., and Cabantchik, Z. I. (2006) Action of chelators in iron-loaded cardiac cells: Accessibility to intracellular labile iron and functional consequences. *Blood 108*, 3195–3203.

(36) Repetto, G., del Peso, A., and Zurita, J. L. (2008) Neutral red uptake assay for the estimation of cell viability/cytotoxicity. *Nat. Protoc. 3*, 1125–1131.

(37) Wang, H., and Joseph, J. A. (1999) Quantifying cellular oxidative stress by dichlorofluorescein assay using microplate reader. *Free Radical Biol. Med. 27*, 612–616.

(38) Lipinski, C. A., Lombardo, F., Dominy, B. W., and Feeney, P. J. (2001) Experimental and computational approaches to estimate solubility and permeability in drug discovery and development settings. *Adv. Drug Delivery Rev. 46*, 3–26.

(39) Buss, J. L., Hermes-Lima, M., and Ponka, P. (2002) Pyridoxal isonicotinoyl hydrazone and its analogues. *Adv. Exp. Med. Biol. 509*, 205–229.

(40) Ponka, P., Richardson, D., Baker, E., Schulman, H. M., and Edward, J. T. (1988) Effect of pyridoxal isonicotinoyl hydrazone and other hydrazones on iron release from macrophages, reticulocytes and hepatocytes. *Biochim. Biophys. Acta 967*, 122–129.

(41) Richardson, D. R., Tran, E. H., and Ponka, P. (1995) The potential of iron chelators of the pyridoxal isonicotinoyl hydrazone class as effective antiproliferative agents. *Blood 86*, 4295–4306.

(42) Sardao, V. A., Oliveira, P. J., Holy, J., Oliveira, C. R., and Wallace, K. B. (2007) Vital imaging of H9c2 myoblasts exposed to tert-butylhydroperoxide: characterization of morphological features of cell death. *BMC Cell Biol. 8*, 11.

(43) Minotti, G. (1989) tert-butyl hydroperoxide-dependent microsomal release of iron and lipid peroxidation. I. Evidence for the reductive release of nonheme, nonferritin iron. *Arch. Biochem. Biophys. 273*, 137–143.

(44) Hershko, C., Link, G., Konijn, A. M., and Cabantchik, Z. I. (2005) Objectives and mechanism of iron chelation therapy. *Ann. N.Y. Acad. Sci. 1054*, 124–135.

(45) Lim, C. K., Kalinowski, D. S., and Richardson, D. R. (2008) Protection against hydrogen peroxide-mediated cytotoxicity in Friedreich's ataxia fibroblasts using novel iron chelators of the 2-pyridylcarboxaldehyde isonicotinoyl hydrazone class. *Mol. Pharmacol. 74*, 225–235.

(46) Buss, J. L., and Ponka, P. (2003) Hydrolysis of pyridoxal isonicotinoyl hydrazone and its analogs. *Biochim. Biophys. Acta 1619*, 177–186.

(47) Harnsberger, H. F., Cochran, E. L., and Szmant, H. H. (1955) The basicity of hydrazones. *J. Am. Chem. Soc. 77*, 5048–5050.

(48) Cordes, E. H., and Jencks, W. P. (1963) Mechanism of hydrolysis of Schiff bases derived from aliphatic amines. *J. Am. Chem. Soc. 85*, 2843–&.

(49) Kale, A. A., and Torchilin, V. P. (2007) Design, synthesis, and characterization of pH-sensitive PEG-PE conjugates for stimuli-sensitive pharmaceutical nanocarriers: the effect of substitutes at the hydrazone linkage on the ph stability of PEG-PE conjugates. *Bioconjugate Chem. 18*, 363–370.

(50) Galati, G., Chan, T., Wu, B., and O'Brien, P. J. (1999) Glutathione-dependent generation of reactive oxygen species by the peroxidase-catalyzed redox cycling of flavonoids. *Chem. Res. Toxicol. 12*, 521–525.

(51) Han van De, W., Gian, C., Gerd, F., and Oleg, A. R. (1996) Estimation of Caco-2 cell permeability using calculated molecular descriptors. *Quant. Struct.-Act. Relat. 15*, 480–490.

(52) Krarup, L. H., Christensen, I. T., Hovgaard, L., and Frokjaer, S. (1998) Predicting drug absorption from molecular surface properties based on molecular dynamics simulations. *Pharm. Res. 15*, 972–978.

(53) Palm, K., Stenberg, P., Luthman, K., and Artursson, P. (1997) Polar molecular surface properties predict the intestinal absorption of drugs in humans. *Pharm. Res. 14*, 568–571.

(54) Mrkvickova, Z., Kovarikova, P., Klimes, J., Kalinowski, D., and Richardson, D. R. (2007) Development and validation of HPLC-DAD methods for the analysis of two novel iron chelators with potent anticancer activity. *J. Pharm. Biomed. Anal. 43*, 1343–1351.

(55) Stariat, J., Kovarikova, P., Klimes, J., Lovejoy, D. B., Kalinowski, D. S., and Richardson, D. R. (2009) HPLC methods for determination of two novel thiosemicarbazone anti-cancer drugs (N4mT and Dp44mT) in plasma and their application to in vitro plasma stability of these agents. *J. Chromatogr., B 877*, 316–322.

(56) Buss, J. L., Neuzil, J., and Ponka, P. (2004) Oxidative stress mediates toxicity of pyridoxal isonicotinoyl hydrazone analogs. *Arch. Biochem. Biophys. 421*, 1–9.